PHYSICAL REVIEW D VOLUME 24, NUMBER 5 1 SEPTEMBER 1981

Photon structure functions and azimuthal asymmetries in two-photon processes

Atsushi Higuchi and Satoshi Matsuda
Department of Physics, Kyoto University, Kyoto 606, Japan

Jiro Kodaira
Stanford Linear Accelerator Center, Stanford University, Stanford, California 94305
(Received 23 March 1981)

Based on the recently developed framework of Curci, Furmanski, and Petronzio, we derive the photon structure functions in quantum chromodynamics (QCD). Then we perform QCD calculations for the azimuthal asymmetries of jets in two-photon processes. We find that in contrast to the case of lepton-hadron scatterings, the deep-inelastic e^+e^- reaction via two-photon exchange is expected to show cleaner signatures for the azimuthal asymmetries as a result of enhanced QCD effects. We suggest that these will serve as useful tests of QCD.

I. INTRODUCTION

Today quantum chromodynamics (QCD) is regarded as the most promising candidate for the field theory of strong interactions. The quantitative test of QCD has now become one of the most important tasks imposed upon particle physicists. Now that the proof of the factorization of mass singularities is completed,[1] perturbative QCD calculations can be attempted in a wide range of deep-inelastic processes.

Among the most interesting processes is the two-photon collision which appears in e^+e^- colliding experiments.[2] Many authors have studied this process by now.[3-10] In this paper we point out that clean tests of QCD effects are expected to be operative in the two-photon process. This is because the leading behavior, with respect to Q^2, of the photon structure functions is exactly calculable as was first shown correctly by Witten.[4] Also the Weizsäcker-Williams approximation allows us to study the structure functions of the electron as well as those of the photon on equal footing.

First we derive the photon structure functions in the framework developed by Curci, Furmanski, and Petronzio[11] (refered to as CFP). Particularly, our presentation will be helpful in clarifying the parton view of the Q^2 evolution of the photon structure functions. It also exhibits naturally how the factorized collinear mass singularities of the photon structure functions are to be absorbed into the hadronic components of the target photon. After this study on the photon structure functions, we investigate the azimuthal asymmetries of jets in the deep-inelastic e^+e^- scattering, aiming at clean and hopefully critical tests of QCD.

The azimuthal asymmetries in lepton-hadron deep-inelastic scatterings were first studied in the context of QCD effects by Georgi and Politzer.[12] They claimed that the azimuthal asymmetries in the above reactions would provide clean tests of QCD. But it was subsequently shown by Cahn[13] that similar nonzero effects in the azimuthal asymmetries would result from the naive parton model (NPM)[14] by incorporating primordial transverse momentum k_T. Moreover, it was shown by Binétruy and Girardi[15] that it is very difficult to discriminate the QCD effects from the primordial k_T effects since both contribute competitively to the azimuthal asymmetries in the case of the lepton-hadron scatterings. We find that this difficulty arises primarily from the inherent nonperturbative QCD ambiguities remaining in the structure functions of the hadron target.

We show in the present paper that in deep-inelastic e^+e^- scattering via two-photon exchange, where the structure functions of the photon and as a result those of the electron are exactly calculable up to the leading order of $\ln Q^2$, one is free from the above-mentioned ambiguities, and thus can predict the enhanced QCD effects for the azimuthal asymmetries against the background effects due to primordial k_T. We claim that in contrast to those in the lepton-hadron scatterings, the azimuthal asymmetries in the two-photon process could be useful to make clean tests of QCD. In the later sections we present the detailed features of the azimuthal asymmetries in perturbative QCD calculations.

In Sec. II we study the photon structure functions. In Sec. III parton cross sections for our problem are presented. The main results for the azimuthal asymmetries are reported in Sec. IV. In Sec. V we give our conclusions and some remarks. Appendices A and B are included to give formulas for anomalous dimensions and calculations for parton cross sections.

II. PHOTON AND ELECTRON STRUCTURE FUNCTIONS

In this section we derive the photon structure functions to the leading order of $\ln Q^2$ in the CFP framework. Although the obtained results are well known, the recently developed technique of CFP allows us to exhibit very nicely how the factorized collinear mass singularities associated with the pointlike-photon dissociation into a quark-antiquark pair are to be absorbed into the hadronic components of the target photon. We identify the hadronic components as the vector-meson-dominance (VMD) contribution to simplify our arguments. Also one big advantage of the present method is that the justification of the usual procedure of jet calculations, i.e., the convolution of the universal Q^2-dependent structure functions with parton cross sections, can be done very easily in the framework adopted here. With the photon structure functions given, it is straightforward to obtain the structure functions of the electron in terms of the well-known equivalent-photon method due to Weizsäcker-Williams.

Following Ref. 11, we use the lightlike gauge and the minimal-subtraction scheme for dealing with mass singularities.

First we discuss the general method for obtaining the Q^2 dependence of the "structure function of partons". Assume there are several kinds of partons: $\alpha,\beta,\delta,\ldots = q,\bar{q},G,\gamma,\ldots$, where $q,\bar{q}$ stand for quark or antiquark, G for gluon, γ for photon, and indices for flavor and color degrees are suppressed. We denote the structure function of parton α by

$$F_\alpha^B\left(\frac{Q^2}{\mu^2},x,\alpha_s(\mu^2),\alpha_{\rm em},\frac{1}{\epsilon}\right), \tag{2.1}$$

where x is the Bjorken variable of deep-inelastic scattering on parton α. The symbol B means "bare", thus F_α^B contain the mass singularities generated in $4+\epsilon$ dimensions.[11]

Following the procedure shown by CFP, i.e., the two-particle-irreducible-ladder expansion to factorize mass singularities, we define the "renormalized" structure functions $F_\alpha^R((Q^2/\mu^2), x,\alpha_s(\mu^2),\alpha_{\rm em})$ and the "renormalization constants" $\Gamma_{\alpha\beta}(x,\alpha_s(\mu^2),\alpha_{\rm em},1/\epsilon)$ which are related (or defined) to satisfy

$$F_\alpha^B\left(\frac{Q^2}{\mu^2},x,\alpha_s(\mu^2),\alpha_{\rm em},\frac{1}{\epsilon}\right) = \int_0^1 dy\, F_\beta^R\left(\frac{Q^2}{\mu^2},y,\alpha_s(\mu^2),\alpha_{\rm em}\right) \times \int_0^1 dz\, \Gamma_{\beta\alpha}\left(z,\alpha_s(\mu^2),\alpha_{\rm em},\frac{1}{\epsilon}\right)\delta(x-yz). \tag{2.2}$$

Taking the x moments, we obtain

$$F_\alpha^B\left(\frac{Q^2}{\mu^2},N,\alpha_s(\mu^2),\alpha_{\rm em},\frac{1}{\epsilon}\right) = F_\beta^R\left(\frac{Q^2}{\mu^2},N,\alpha_s(\mu^2),\alpha_{\rm em}\right)\Gamma_{\beta\alpha}\left(N,\alpha_s(\mu^2),\alpha_{\rm em},\frac{1}{\epsilon}\right). \tag{2.3}$$

Since F_α^B, as introduced in Ref. 11, is a bare quantity and does not depend on μ, we should have

$$\mu\frac{d}{d\mu}F_\alpha^B=0 \tag{2.4}$$

and

$$\left(\mu\frac{d}{d\mu}F_\beta^R\right)\Gamma_{\beta\alpha}+F_\beta^R\left(\mu\frac{d}{d\mu}\Gamma_{\beta\alpha}\right)=0. \tag{2.5}$$

Therefore,

$$\mu\frac{d}{d\mu}F_\alpha^R-\gamma_{\beta\alpha}F_\beta^R=0, \tag{2.6}$$

where

$$\gamma_{\beta\alpha}\equiv-\left(\mu\frac{d}{d\mu}\Gamma_{\beta\delta}\right)(\Gamma^{-1})_{\delta\alpha}. \tag{2.7}$$

The total derivative over μ is given by

$$\mu\frac{d}{d\mu}=\mu\frac{\partial}{\partial\mu}+\beta(g_s,\epsilon)\frac{\partial}{\partial g_s}+\beta_{\rm em}(e,\epsilon)\frac{\partial}{\partial e}, \tag{2.8}$$

where

$$\beta(g_s,\epsilon)=\beta(g_s)+\tfrac{1}{2}\epsilon g_s \tag{2.9}$$

and

$$\beta_{\rm em}(e,\epsilon)=\beta_{\rm em}(e)+\tfrac{1}{2}\epsilon e \tag{2.10}$$

are the Peterman–Stueckelberg–Gell-Mann–Low[16] β functions in $4+\epsilon$ dimensions.

In the following we only consider the case of lowest order in $\alpha_{\rm em}$, so, taking the limit $\epsilon\to 0$, we obtain from (2.6) and (2.8)

$$\left(\mu\frac{\partial}{\partial\mu}+\beta(g_s)\frac{\partial}{\partial g_s}\right)F_\alpha^R=F_\beta^R\gamma_{\beta\alpha}, \tag{2.11}$$

where from (2.7) we have

$$\gamma_{\beta\alpha}(N,\alpha_s(\mu),\alpha_{\rm em}) = -\left(\beta(g_s,\epsilon)\frac{\partial}{\partial g_s}+\beta_{\rm em}(e,\epsilon)\frac{\partial}{\partial e}\right)\Gamma_{\beta\delta}(\Gamma^{-1})_{\delta\alpha}, \tag{2.12}$$

since $\Gamma_{\alpha\beta}$ does not have explicit μ dependence.

Solving (2.11) we obtain

$$F_\alpha^R\left(\frac{Q^2}{\mu^2}, N, \alpha_s(\mu^2), \alpha_{\rm em}\right) = F_\beta^R(1, N, \alpha_s(Q^2), \alpha_{\rm em})\left[T^* \exp\left(\int_{g_s(Q^2)}^{g_s(\mu^2)} \frac{\vec{\gamma}(g)}{\beta(g)}\, dg\right)\right]_{\beta\alpha}, \tag{2.13}$$

where the T^* ordering is defined by

$$T^* \exp\left[\int_a^b \vec{f}(t)dt\right] \equiv \sum_{n=0}^{\infty} \int_a^b dt_n \int_a^{t_n} dt_{n-1} \cdots \int_a^{t_2} dt_1 \vec{f}(t_1)\vec{f}(t_2)\cdots\vec{f}(t_n), \tag{2.14}$$

and $\alpha_s(Q^2) = \alpha_s(Q^2/\mu^2, \alpha_s(\mu^2))$ satisfies

$$\left(\mu\frac{\partial}{\partial\mu} + \beta(g_s)\frac{\partial}{\partial g_s}\right)\alpha_s(Q^2) = 0. \tag{2.15}$$

In the lowest order of $\alpha_{\rm em}$ the anomalous-dimension matrix is effectively given by

$$\vec{\gamma} = \begin{pmatrix} \vec{\gamma}_s & \vec{\gamma}_{s\gamma} \\ \vec{0} & 0 \end{pmatrix} = \begin{pmatrix} \vec{\gamma}_{q^i q^j} & \vec{\gamma}_{q^i G} & \vec{\gamma}_{q^i\gamma} \\ \vec{\gamma}_{Gq^j} & \gamma_{GG} & \gamma_{G\gamma} \\ \vec{0} & 0 & 0 \end{pmatrix}, \tag{2.16}$$

because the γ's of the bottom row are at most $O(\alpha_{\rm em})$ and couple to functions of $O(\alpha_{\rm em})$, and therefore start to contribute only to the part of $O(\alpha_{\rm em}^2)$. Substituting (2.16), we get

$$\left[T^* \exp\left(\int_{g_s(Q^2)}^{g_s(\mu^2)} \frac{\vec{\gamma}(g)}{\beta(g)}\, dg\right)\right]_{\beta\alpha} = \begin{pmatrix} T^* \exp\left[\int_{g_s(Q^2)}^{g_s(\mu^2)} \frac{\vec{\gamma}_s(g)}{\beta(g)}\, dg\right] & \int_{g_s(Q^2)}^{g_s(\mu^2)} dg'\, T^* \exp\left[\int_{g_s(Q^2)}^{g'} \frac{\vec{\gamma}_s(g)}{\beta(g)}\, dg\right] \frac{\vec{\gamma}_{s\gamma}(g')}{\beta(g')} \\ \vec{0} & 1 \end{pmatrix}. \tag{2.17}$$

We define the renormalized Q^2-dependent structure functions $f_{\beta\alpha}^R((Q^2/\mu^2), x)$ by

$$\int_0^1 dx\, x^{N-1} f_{\beta\alpha}^R\left(\frac{Q^2}{\mu^2}, x\right) \equiv \left[T^* \exp\left(\int_{g_s(Q^2)}^{g_s(\mu^2)} \frac{\gamma(g)}{\beta(g)}\, dg\right)\right]_{\beta\alpha}. \tag{2.18}$$

Then we have

$$F_\alpha^R\left(\frac{Q^2}{\mu^2}, x, \alpha_s(\mu^2), \alpha_{\rm em}\right) = \int_0^1 dy\, F_\beta^R(1, y, \alpha_s(Q^2), \alpha_{\rm em}) \int_0^1 dz\, f_{\beta\alpha}^R\left(\frac{Q^2}{\mu^2}, z\right)\delta(x - yz). \tag{2.19}$$

Finally, defining $f_{\beta\alpha}^B((Q^2/\mu^2), x, \alpha_s(\mu^2), \alpha_{\rm em}, (1/\epsilon))$ by

$$f_{\beta\alpha}^B\left(\frac{Q^2}{\mu^2}, x, \alpha_s(Q^2), \alpha_{\rm em}, \frac{1}{\epsilon}\right) = \int_0^1 dy\, f_{\beta\delta}^R\left(\frac{Q^2}{\mu^2}, y\right) \int_0^1 dz\, \Gamma_{\delta\alpha}\left(z, \alpha_s(\mu^2), \alpha_{\rm em}, \frac{1}{\epsilon}\right)\delta(x - yz), \tag{2.20}$$

we obtain

$$F_\alpha^B\left(\frac{Q^2}{\mu^2}, x, \alpha_s(\mu^2), \alpha_{\rm em}, \frac{1}{\epsilon}\right) = \int_0^1 dy\, F_\beta^R(1, y, \alpha_s(Q^2), \alpha_{\rm em}) \int_0^1 dz\, f_{\beta\alpha}^B\left(\frac{Q^2}{\mu^2}, z, \alpha_s(\mu^2), \alpha_{\rm em}, \frac{1}{\epsilon}\right)\delta(x - yz). \tag{2.21}$$

It is to be noted that in (2.19) and (2.21) the structure function is factorized into the hard-parton cross section $F_\beta^R(1, y, \alpha_s(Q^2), \alpha_{\rm em})$ and the universal Q^2-dependent parton structure function $f_{\beta\alpha}^B$. By the usual procedure the outgoing partons encountered in calculating $F_\beta^R(1, y, \alpha_s(Q^2), \alpha_{\rm em})$ can be identified as exclusive jets. Then, if we are interested in the generalized structure functions $F_\alpha^B(Q^2/\mu^2, x, w\text{'s}, \alpha_s(Q^2), \alpha_{\rm em}, 1/\epsilon)$ including the jet variables w's which describe jets produced in the final state of deep-inelastic scattering on parton α, we just substitute $F_\beta^R(1, y, \alpha_s(Q^2), \alpha_{\rm em})$ by the exclusive parton cross section $F_\beta^R(1, y, w\text{'s}, \alpha_s(Q^2), \alpha_{\rm em})$ in (2.21). In this way we obtain

$$F_\alpha^B\left(\frac{Q^2}{\mu^2}, x, w\text{'s}, \alpha_s(Q^2), \alpha_{\rm em}, \frac{1}{\epsilon}\right) = \int_0^1 dy\, F_\beta^R(1, y, w\text{'s}, \alpha_s(Q^2), \alpha_{\rm em}) \int_0^1 dz\, f_{\beta\alpha}^B\left(\frac{Q^2}{\mu^2}, z, \alpha_s(\mu^2), \alpha_{\rm em}, \frac{1}{\epsilon}\right)\delta(x - yz). \tag{2.22}$$

When the target is a usual hadron h, we define its Q^2-dependent structure function by the convolution

$$f_{ah}(x,Q^2)=\int_0^1 dy\, f_{ab}^B\left(\frac{Q^2}{\mu^2},y,\alpha_s(\mu^2),0,\frac{1}{\epsilon}\right)\int_0^1 dz f_{bh}^B\left(z,\frac{1}{\epsilon}\right)\delta(x-yz), \tag{2.23}$$

where the subscripts a, b stand for q, $\bar{q}$, and G, and $f_{ah}^B(x,(1/\epsilon))$ is the bare parton density in the hadron. $f_{ah}(x,Q^2)$ can also be expressed as

$$f_{ah}(x,Q^2)=\int_0^1 dy\, f_{ab}^R\left(\frac{Q^2}{\mu^2},y\right)\int_0^1 dz\, f_{bh}^R(z)\delta(x-yz), \tag{2.24}$$

where

$$f_{ah}^R(x)=\int_0^1 dy\,\Gamma_{ab}\left(y,\alpha_s(\mu^2),0,\frac{1}{\epsilon}\right)\times\int_0^1 dz\, f_{bh}^B\left(z,\frac{1}{\epsilon}\right)\delta(x-yz). \tag{2.25}$$

$f_{ah}(x,Q^2)$, or equivalently $f_{ah}^R(x)$, must be finite according to the Kinoshita-Lee-Nauenberg theorem.[17,18] From (2.22) we thus get the usual procedure of convoluting the Q^2-dependent structure functions with parton cross sections,

$$F_h\left(\frac{Q^2}{\mu^2},x,w\text{'s},\alpha_s(\mu^2)\right)=\int_0^1 dy\, F_a^R(1,y,w\text{'s},\alpha_s(Q^2),0)\times\int_0^1 dz\, f_{ah}(z,Q^2)\delta(x-yz). \tag{2.26}$$

In the case of a photon target, the situation is somewhat different. The target photon "γ" has the bare parton densities

$$f_{\alpha\text{"}\gamma\text{"}}^B\left(x,\frac{1}{\epsilon}\right)=\delta(1-x)\delta_{\alpha\gamma}+f_{\alpha\text{"}\gamma\text{"}}^{B(\mathrm{VMD})}\left(x,\frac{1}{\epsilon}\right)+O(\alpha_{\mathrm{em}}{}^2), \tag{2.27}$$

where the first term represents the contribution of the target photon acting as a bare parton γ, while the second stands for the hadronic components inside the target photon which are typified by the VMD contribution. Also we note that in the CFP framework we have

$$\Gamma_{\gamma\gamma}\left(x,\frac{1}{\epsilon}\right)=\delta(1-x)+O(\alpha_{\mathrm{em}}{}^2). \tag{2.28}$$

Then, convoluting (2.27) with (2.20) and using (2.28), we obtain the finite Q^2-dependent structure functions of the target photon "γ":

$$f_{a\text{"}\gamma\text{"}}(x,Q^2)=f_{a\gamma}^R\left(\frac{Q^2}{\mu^2},x\right)+\int_0^1 dy\, f_{ab}^R\left(\frac{Q^2}{\mu^2},y\right)\int_0^1 dz f_{b\text{"}\gamma\text{"}}^{R(\mathrm{VMD})}(z)\delta(x-yz)+O(\alpha_{\mathrm{em}}{}^2), \tag{2.29}$$

where a and b denote q, $\bar{q}$, and G, and the renormalized parton densities $f_{a\text{"}\gamma\text{"}}^{R(\mathrm{VMD})}$ corresponding to the VMD component of the target photon is given by

$$f_{a\text{"}\gamma\text{"}}^{R(\mathrm{VMD})}(x)=\Gamma_{a\gamma}\left(x,\alpha_s(\mu^2),\alpha_{\mathrm{em}},\frac{1}{\epsilon}\right)+\int_0^1 dy\,\Gamma_{ab}\left(y,\alpha_s(\mu^2),0,\frac{1}{\epsilon}\right)\times\int_0^1 dz\, f_{b\text{"}\gamma\text{"}}^{B(\mathrm{VMD})}\left(z,\frac{1}{\epsilon}\right)\delta(x-yz). \tag{2.30}$$

This result exhibits explicitly the manner in which the collinear mass singularities associated with the "renormalization constants" $\Gamma_{a\gamma}(x,\alpha_s(\mu^2),\alpha_{\mathrm{em}},1/\epsilon)$ are absorbed into the hadronic components of the target photon.

Following Ref. 11, we now calculate Γ's. It is straightforward to obtain the Γ's to the order needed to get the leading behavior of F_γ^B. The results are

$$\begin{aligned}
\Gamma_{qq}(x)&=\delta(1-x)+\frac{2}{\epsilon}\frac{\alpha_s(\mu)}{2\pi}P_{qq}(x),\\
\Gamma_{qG}(x)&=\frac{2}{\epsilon}\frac{\alpha_s(\mu)}{2\pi}P_{qG}(x),\\
\Gamma_{Gq}(x)&=\frac{2}{\epsilon}\frac{\alpha_s(\mu)}{2\pi}P_{Gq}(x),\\
\Gamma_{GG}(x)&=\delta(1-x)+\frac{2}{\epsilon}\frac{\alpha_s(\mu)}{2\pi}P_{GG}(x),
\end{aligned} \tag{2.31}$$

where the P's are the well-known Altarelli-Parisi[19] probability functions and

$$\Gamma_{q\gamma}(x)=\frac{2}{\epsilon}\frac{\alpha_{\mathrm{em}}}{2\pi}[x^2+(1-x)^2]. \tag{2.32}$$

The other Γ's may be set equal to zero. Taking the x moments of (2.31) and (2.32), we get γ's from (2.7). Since the obtained γ's turn out to be the same as the anomalous dimensions appearing in the operator-product expansion (OPE), we substitute them into (2.17) and obtain the following known results from (2.18):

$$\int_0^1 dx\, x^{N-1} f^R_{q^i q^j}\left(x, \frac{Q^2}{\mu^2}\right) = \left(\delta_{ij} - \frac{1}{2f}\right)\left(\frac{\alpha_s(Q^2)}{\alpha_s(\mu^2)}\right)^{d_N^{\rm NS}} + \frac{1}{2f}\left[\frac{d_N^+ - d_N^{GG}}{d_N^+ - d_N^-}\left(\frac{\alpha_s(Q^2)}{\alpha_s(\mu^2)}\right)^{d_N^+} + \frac{d_N^{GG} - d_N^-}{d_N^+ - d_N^-}\left(\frac{\alpha_s(Q^2)}{\alpha_s(\mu^2)}\right)^{d_N^-}\right],$$

$$\int_0^1 dx\, x^{N-1} f^R_{q^i G}\left(x, \frac{Q^2}{\mu^2}\right) = \frac{1}{2f}\,\frac{d_N^{qG}}{d_N^+ - d_N^-}\left[\left(\frac{\alpha_s(Q^2)}{\alpha_s(\mu^2)}\right)^{d_N^-} - \left(\frac{\alpha_s(Q^2)}{\alpha_s(\mu^2)}\right)^{d_N^+}\right],$$

$$\int_0^1 dx\, x^{N-1} f^R_{Gq^i}\left(x, \frac{Q^2}{\mu^2}\right) = \frac{d_N^{Gq}}{d_N^+ - d_N^-}\left[\left(\frac{\alpha_s(Q^2)}{\alpha_s(\mu^2)}\right)^{d_N^-} - \left(\frac{\alpha_s(Q^2)}{\alpha_s(\mu^2)}\right)^{d_N^+}\right], \tag{2.33}$$

$$\int_0^1 dx\, x^{N-1} f^R_{GG}\left(x, \frac{Q^2}{\mu^2}\right) = \frac{d_N^+ - d_N^{GG}}{d_N^+ - d_N^-}\left(\frac{\alpha_s(Q^2)}{\alpha_s(\mu^2)}\right)^{d_N^-} + \frac{d_N^{GG} - d_N^-}{d_N^+ - d_N^-}\left(\frac{\alpha_s(Q^2)}{\alpha_s(\mu^2)}\right)^{d_N^+}$$

and

$$\int_0^1 dx\, x^{N-1} f^R_{q^i\gamma}\left(x, \frac{Q^2}{\mu^2}\right) = \frac{3\alpha_{\rm em}}{2\pi}\ln\frac{Q^2}{\Lambda^2}\, d_N^{q\gamma}\left[(e_i^2 - \langle e^2\rangle)\,\frac{1}{1+d_N^{\rm NS}} + \langle e^2\rangle\,\frac{1+d_N^{GG}}{K_N}\right],$$

$$\int_0^1 dx\, x^{N-1} f^R_{G\gamma}\left(x, \frac{Q^2}{\mu^2}\right) = 2f\,\frac{3\alpha_{\rm em}}{2\pi}\ln\frac{Q^2}{\Lambda^2}\, d_N^{q\gamma}\langle e^2\rangle\,\frac{d_N^{Gq}}{K_N}, \tag{2.34}$$

where f is the number of flavors, K_N is

$$K_N = 1 + d_N^{\rm NS} + d_N^{GG} + d_N^{\rm NS} d_N^{GG} - d_N^{qG} d_N^{Gq}, \tag{2.35}$$

and d's are given in Appendix A.

Now from (2.29) we have

$$f_{a\text{"}\gamma\text{"}}(x, Q^2) = f^R_{a\gamma}\left(\frac{Q^2}{\mu^2}, x\right) + f^{\rm VMD}_{a\text{"}\gamma\text{"}}(x, Q^2) \tag{2.36}$$

with

$$f^{\rm VMD}_{a\text{"}\gamma\text{"}}(x, Q^2) = \int_0^1 dy\, f^R_{ab}\left(\frac{Q^2}{\mu^2}, y\right)\int_0^1 dz\, f^{R({\rm VMD})}_{b\text{"}\gamma\text{"}}(z)\,\delta(x - yz) \tag{2.37}$$

and $a, b = q, \bar{q}, G$. Since in (2.33) and (2.34) all d's are positive, we find that for very large Q^2 the second term due to VMD is suppressed. So the photon structure function $F_{a\text{"}\gamma\text{"}}(x, Q^2)$ is dominated by the photon-parton contribution $f^R_{a\gamma}(Q^2/\mu^2, x)$ which is exactly given by (2.34). We observe that this leading contribution behaves like $\ln Q^2$. Performing the inverse Mellin transformation from (2.34), we obtain the x dependence of $f^R_{a\gamma}(Q^2/\mu^2, x)$. We present our results for three flavors (see Fig. 1). For the case of four flavors, refer to Ref. 9.

Although $f^{\rm VMD}_{a\text{"}\gamma\text{"}}$ is expected to be smaller than the next-to-leading order correction of $f^R_{a\gamma}$ in the $Q^2 \to \infty$ limit, in the following analysis at large but finite Q^2 we include $f^{\rm VMD}_{a\text{"}\gamma\text{"}}$, particularly to estimate the possible nonperturbative contribution of primordial k_T to the angular asymmetries. On the other hand we expect that the next-to-leading order correction to the distribution functions will not affect substantially the angular asymmetries because the latter mainly reflect the characteristics of parton cross sections but not of the distribution function.

$f^{\rm VMD}_{a\text{"}\gamma\text{"}}$ is basically unknown in the present scheme since $f^{R({\rm VMD})}_{b\text{"}\gamma\text{"}}(z)$ is not given in (2.37). Therefore we use for these parts the vector-dominance model and assume simple structure functions for vector mesons as many authors do.[4,6,9] Moreover we neglect the gluon distribution from the vector-dominance model and the Q^2 dependence in the assumed structure functions. This simplification is valid for our present study since our point here is to show explicitly that their corrections do *not*

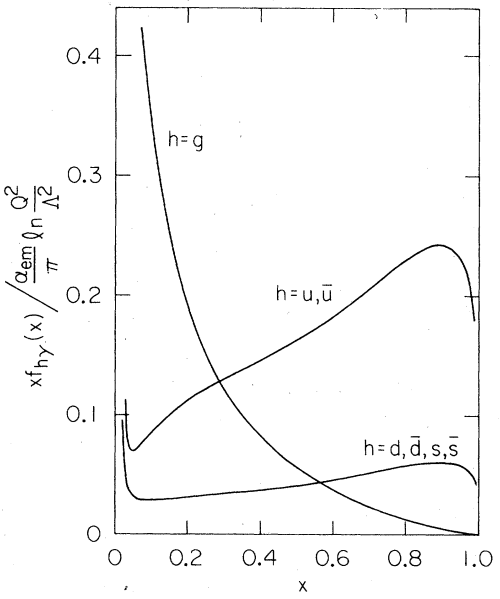

FIG. 1. The photon structure functions with three quark flavors.

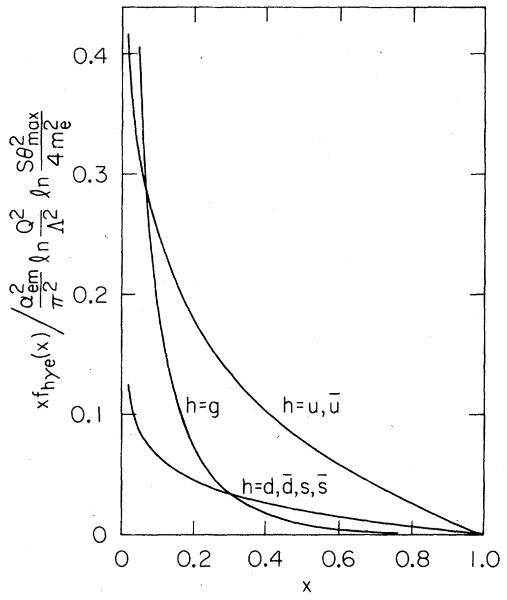

FIG. 2. The electron structure functions with three quark flavors.

spoil the characteristic signatures of the leading QCD effects for the azimuthal asymmetries.

For $f_{q^i/\gamma''}^{\mathrm{VMD}}(x)$ we get by the vector-dominance model

$$f_{q^i/\gamma''}^{\mathrm{VMD}}(x)=\sum_V \frac{4\pi\alpha_{\mathrm{em}}}{f_V{}^2} f_{q^i/V}(x) \simeq \frac{4\pi\alpha_{\mathrm{em}}}{f_\rho{}^2} f_{q^i/\rho}(x). \tag{2.38}$$

From the experimental value of $\Gamma_{\rho^0\to e^+e^-}$ we obtain roughly

$$\frac{f_\rho{}^2}{4\pi} \approx 2.$$

Assuming $f_{q^i/\rho^0} \propto (1-x)/x$ and 50% of the gluon component, we finally get

$$f_{q^i/\gamma''}^{\mathrm{VMD}}(x) \simeq \frac{\alpha_{\mathrm{em}}}{2}\langle x\rangle_{q^i}\frac{1-x}{x}, \tag{2.39}$$

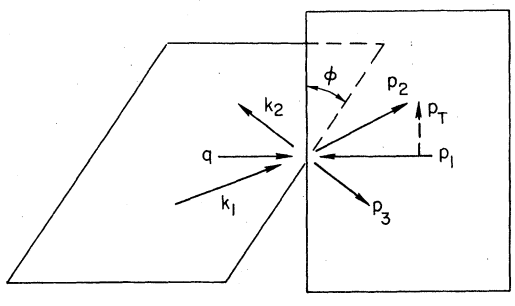

FIG. 3. Kinematics. k_1 and k_2 are the momenta for incident and outgoing electrons which couple to the virtual photon. p_1 is the momentum of the incident parton. p_2 and p_3 are the momenta of the scattered partons.

where the average momentum $\langle x\rangle_{q^i}$ carried by the quarks inside ρ^0 is taken to be

$$\langle x\rangle_{q^i}=\begin{cases}0.25 \text{ for } u,\bar{u},d,\bar{d}\\ 0 \text{ for } s,\bar{s},c,\bar{c}\end{cases}. \tag{2.40}$$

It is rather a rough estimation but sufficient for our purpose.

The electron structure function is obtained using the equivalent photon approximation. Since we restrict ourselves to the single tag events, we should use the following form of the equivalent-photon spectrum (in the leading approximation):

$$\frac{dN}{dx}=\frac{\alpha_{\mathrm{em}}}{2\pi}\ln\frac{s\theta_{\max}{}^2}{4m_e{}^2}\frac{1+(1-x)^2}{x}, \tag{2.41}$$

where x is not too close to 0 or 1, and the electron is constrained to lie inside a cone of half-angle $\theta_{\max}$. By the convolution

$$f_{ae}(x,Q^2)=\int_x^1 \frac{dz}{z}\frac{dN}{dz} f_{a''\gamma''}\left(\frac{x}{z},Q^2\right), \tag{2.42}$$

we get the structure functions of the electron.

The results of the leading QCD part are shown in Fig. 2 for three flavors. For the VMD part we can obtain the results from (2.39), simply replacing the factor $(1-x)/x$ by

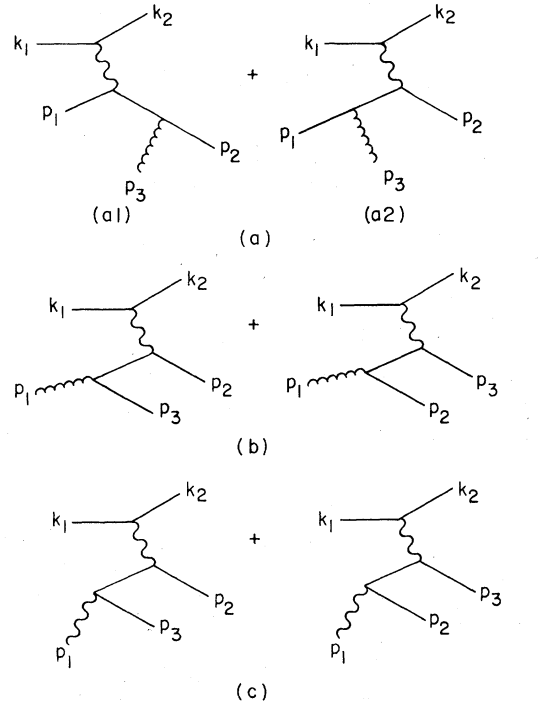

FIG. 4. The Feynman graphs for parton cross section. (a) Electron-quark scattering. (b) Electron-gluon scattering. (c) Electron-photon scattering.

$$\frac{\alpha_{em}}{\pi}\ln\frac{s\theta_{max}^2}{4m_e^2}\left[\frac{1}{x}\left(\ln\frac{1}{x}-\frac{7}{4}\right)+\frac{3}{2}+\ln\frac{1}{x}+\frac{x}{4}\right]. \tag{2.43}$$

III. PARTON CROSS SECTION

Now we calculate the parton cross sections which we need for our purpose. The kinematics are shown in Fig. 3 and the contributing diagrams are given in Fig. 4. We introduce the usual variables

$$x_p=\frac{Q^2}{2p_1\cdot q},\quad y=\frac{p_1\cdot q}{p_1\cdot k_1},\quad z_p=\frac{p_1\cdot p_2}{p_1\cdot q},\quad \phi,\ p_T \tag{3.1}$$

where $q=k_1-k_2$, $Q^2\equiv -q^2$ and, as illustrated in Fig. 3, the azimuthal angle ϕ and the transverse momentum p_T are defined in the frame where $\vec{q}\|\vec{p}_1$. The results are[20]

$$\frac{d\sigma_i}{dx_p dy\,dz_p dp_T^2 d\phi}=\alpha_s(Q^2)\frac{\alpha_{em}^2}{2\pi Q^2 y}e_q^2\delta\left(p_T^2-\frac{Q^2z_p(1-z_p)(1-x_p)}{x_p}\right)c_i(A_i+B_i\cos\phi+C_i\cos 2\phi), \tag{3.2}$$

where e_q is the charge of the quark hit by the hard photon with momentum q. The subscript $i=(a),(b)$ stands for the diagrams (a1)+(a2), (b1)+(b2) of Fig. 4,

$$c_{(a)}=C_2(R)=\tfrac{4}{3},\quad c_{(b)}=T(R)=\tfrac{1}{2},$$

and A_i, B_i, and C_i are given as follows:[20]

$$A_{(a)}=8(1-y)x_pz_p+[1+(1-y)^2]\left[(1-x_p)(1-z_p)+\frac{1+x_p^2z_p^2}{(1-x_p)(1-z_p)}\right], \tag{3.3a}$$

$$A_{(b)}=16(1-y)x_p(1-x_p)+[1+(1-y)^2][x_p^2+(1-x_p)^2]\frac{z_p^2+(1-z_p)^2}{z_p(1-z_p)}, \tag{3.3b}$$

$$B_{(a)}=-4(2-y)(1-y)^{1/2}\left[\frac{x_pz_p}{(1-x_p)(1-z_p)}\right]^{1/2}\times[x_pz_p+(1-x_p)(1-z_p)], \tag{3.4a}$$

$$B_{(b)}=-4(2-y)(1-y)^{1/2}\left[\frac{x_p(1-x_p)}{z_p(1-z_p)}\right]^{1/2}\times(1-2x_p)(1-2z_p), \tag{3.4b}$$

$$C_{(a)}=4(1-y)x_pz_p, \tag{3.5a}$$

$$C_{(b)}=8(1-y)x_p(1-z_p). \tag{3.5b}$$

Replacing $\alpha_s(Q^2)$ by $\alpha_{em}e_q^2$ and the color factor $C_{(b)}$ by $C_{(c)}=3$ in the formulas of Fig. 4(b), we get the cross section for the diagrams Fig. 4(c) with

$$A_{(c)}=A_{(b)},\quad B_{(c)}=B_{(b)},\quad C_{(c)}=C_{(b)}. \tag{3.6}$$

Since experimentally we are not yet in a position to distinguish quark jets from gluon jets nor from antiquark jets, we should find an alternative way of defining the direction of the hadron plane. Suppose we require z_p to be larger than $\frac{1}{2}$. Then the sense of the direction of the hadron plane is redefined in terms of the "more energetic jet" axis. With the definition (3.1) we have

$$\frac{p_1\cdot p_3}{p_1\cdot q}=1-z_p. \tag{3.7}$$

Then we introduce the following newly defined z_p':

$$z_p'\equiv\max\left\{\frac{p_1\cdot p_2}{p_1\cdot q},\frac{p_1\cdot p_3}{p_1\cdot q}\right\},\quad \tfrac{1}{2}<z_p'<1. \tag{3.8}$$

The corresponding B_i''s are obtained from (3.4) by noting the sign change in the substitution $z_p\to 1-z_p$, $\phi\to\pi+\phi$:

$$B'_{(a)}=-4(2-y)(1-y)^{1/2}\left(\frac{x_p}{1-x_p}\right)^{1/2}\times x_p\left[\left(\frac{z_p'}{1-z_p'}\right)^{1/2}z_p'-\left(\frac{1-z_p'}{z_p'}\right)^{1/2}(1-z_p')\right], \tag{3.4a'}$$

$$B'_{(b)}=-8(2-y)(1-y)^{1/2}[x_p(1-x_p)]^{1/2}\times(2x_p-1)\left[\left(\frac{z_p'}{1-z_p'}\right)^{1/2}-\left(\frac{1-z_p'}{z_p'}\right)^{1/2}\right], \tag{3.4b'}$$

where z_p' is constrained to the region

$$\tfrac{1}{2}<z_p'<1. \tag{3.9}$$

It is to be noted here that $B_{(a)}$ and $B'_{(a)}$ are always negative and that this fact is characteristic of the vector coupling of gluons. If we calculate with scalar gluons, we obtain

$$B_{(a),\,scalar}\propto 2(2-y)(1-y)^{1/2}\left[\frac{x_pz_p}{(1-x_p)(1-z_p)}\right]^{1/2}\times[x_p(1-z_p)+(1-x_p)z_p], \tag{3.10}$$

$$B'_{(a),\,scalar}\propto 2(2-y)(1-y)^{1/2}[x_p(1-x_p)]^{1/2}\times\left[\left(\frac{z_p'}{1-z_p'}\right)^{1/2}z_p'-\left(\frac{1-z_p'}{z_p'}\right)^{1/2}(1-z_p')\right],\quad (\tfrac{1}{2}<z_p'<1). \tag{3.10'}$$

$B_{(a),\text{scalar}}$ and $B'_{(a),\text{scalar}}$ are always positive. It should be noted that the sum of direct terms [i.e., $|(a1)|^2 + |(a2)|^2$ in Fig. 4a] has essentially the same structure in both cases of the scalar and the vector couplings, and the difference comes from the interference terms. This means that the negative definiteness of B_a and B'_a is not at all a trivial kinematical result and that it is very important to observe it for the test of perturbative QCD.

The details of the above calculations are given in Appendix B. Finally we present the parton cross section with primordial k_T in the framework of the NPM[13]:

$$\frac{d\sigma}{dx_p dy\, dz_p dp_T^2 d\phi} = \frac{\alpha_{\text{em}}^2 e_q^2}{Q^2 y}\left[\left(1+2\frac{k_T^2}{Q^2}\right)[1+(1-y)^2]+8(1-y)\frac{k_T^2}{Q^2} - 4\frac{k_T^2}{Q}(2-y)(1-y)^{1/2}\cos\phi + 4\frac{k_T^2}{Q^2}(1-y)\cos 2\phi\right]\delta(1-x_p)\delta(1-z_p)\delta(p_T^2-k_T^2). \tag{3.11}$$

IV. AZIMUTHAL ASYMMETRIES

It is a straightforward problem of convolution to get the azimuthal asymmetry formulas for $\langle\cos\phi\rangle$ and $\langle\cos 2\phi\rangle$. We regard partons as jets and measure ϕ with regard to "the more energetic jet," that is, the jet with the larger z_{jet}. Thus the z_{jet} of "the more energetic jet" may be identified as the z'_p introduced by (3.8) in the previous section.

Since typical three-jet events are expected to be rare in the Q^2 region where we have a sufficient number of events, some well-defined procedure should be used to determine the hadron plane and ϕ experimentally. The most natural one is as follows (see Fig. 5):

(1) Choose a Lorentz frame where the virtual photon is parallel to the target electron (or positron), e.g., the c.m. frame of the virtual photon and the electron (positron).

(2) Determine the hadron plane so as to minimize the acoplanarity[21] with respect to the outgoing hadrons under the condition that the chosen plane should include the axis of the virtual photon and the target electron (or positron).

(3) Divide the outgoing hadrons into two groups (jets) by another plane including the above axis and being perpendicular to the hadron plane.

(4) Calculate z_{jet} for each group as

$$z_{\text{jet}} = \frac{P\cdot(\sum_i k^{(i)})}{P\cdot q}, \tag{4.1}$$

where P is the momentum of the target electron (or positron).

(5) Determine the angle ϕ between the lepton plane and the half of the hadron plane containing the group (jet) with the larger z_{jet}.

We present the results for the electron structure functions with three flavors because the charm contribution is expected to be suppressed due to its large mass in most of the Q^2 range considered here.[22] Even if we have the charm contribution at very large Q^2, its effect results in the increase of the cross sections, but does not affect very much the characteristics of the effective ratios of the cross sections such as $\langle\cos\phi\rangle$ and $\langle\cos 2\phi\rangle$.

We calculate the azimuthal asymmetries with fixed Q^2 and x_H at a given $s = (100\ \text{GeV})^2$, using the following formula:

$$\langle\cos\phi\rangle_{x_H,Q^2} = \left[\sum_i \int d\xi\, dx_p\, dz_{\text{jet}}\, dp_T^2 d\phi\, \cos\phi\, \frac{d\sigma_i}{dx_p dQ^2 dz_{\text{jet}}\, dp_T^2 d\phi} f_{ie}(\xi,Q^2)\delta(x_H-\xi x_p)\right] \Big/ \frac{d\sigma^{(0)}}{dx_H dQ^2}, \tag{4.2}$$

where $d\sigma^{(0)}$ is the cross section in the leading order of $\ln Q^2$, and i stands for a parton (q, $\bar{q}$, G, and γ). f_{ae} ($a = q, \bar{q}, G$) was introduced by (2.42), whereas $f_{\gamma e}$ is equal to dN/dx defined by (2.41) and contributes to the "direct photon" process which will be discussed later. The formula for $\langle\cos 2\phi\rangle_{x_H,Q^2}$ can be obtained replacing $\cos\phi$ by $\cos 2\phi$ in the above Eq. (4.2). We have used the relation

$$Q^2 = x_H y s \tag{4.3}$$

and put $\Lambda = 500$ MeV.

To compare our results with those of the naive parton model (NPM), we estimate the latter by assuming the following primodial k_T distribution in the VMD part of the photon structure functions and using (3.11):

$$f(k_T)2\pi k_T dk_T = \frac{1}{\pi\langle k_T^2\rangle} e^{-(k_T^2/\langle k_T^2\rangle)} 2\pi k_T dk_T. \tag{4.4}$$

There is no room for this kind of k_T in the leading

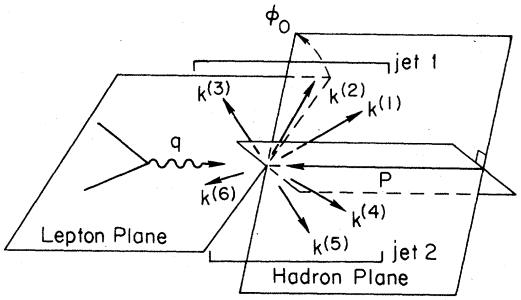

$$z_{jet1} \equiv \frac{P\cdot(k^{(1)}+k^{(2)}+k^{(3)})}{P\cdot q}$$

$$z_{jet2} \equiv \frac{P\cdot(k^{(4)}+k^{(5)}+k^{(6)})}{P\cdot q}$$

$$z_{jet1} > z_{jet2} \longrightarrow \phi = \phi_0$$

$$z_{jet1} < z_{jet2} \longrightarrow \phi = \phi_0 + \pi$$

FIG. 5. The experimental determination of ϕ.

part of the photon structure functions which is proportional to $\ln Q^2/\Lambda^2$. For numerical purposes we take $\langle k_T^2\rangle = (400\ \text{MeV})^2$ as in Ref. 15.[23]

We remind you here that in the contributions to the azimuthal asymmetries there are the direct-photon processes shown in Fig. 4(c) besides the perturbative QCD processes corresponding to Figs. 4(a) and 4(b). The direct-photon contributions turn out to be substantially large. They are backgrounds when we want to detect the azimuthal asymmetries as a QCD effect. But we emphasize that these QED contributions are calculable without ambiguity and enter as theoretically well-determined quantities. In fact, their experimental detection is itself an interesting problem.

We should not forget that hadrons in a jet are expected to be distributed symmetrically around the jet axis with the average p_T of about 300 MeV. This p_T spread works to diminish the azimuthal asymmetries. The best method to take this effect into account is to perform the Monte Carlo simulation used in jet analyses, but here we simply adopt the p_T cutoff method as a substitute for the elaborate Monte Carlo simulation. We present the results with a simple p_T cutoff of the jet momentum requiring $p_T \geq 300$ MeV as well as those without p_T cutoff.

We show the x_H dependence of the azimuthal asymmetries for $Q^2 = 5$ and 25 GeV^2 in Figs. 6–11. The QCD as well as direct-photon contributions to $\langle\cos\phi\rangle$ are sensitive to the p_T cutoff (compare Figs. 6 and 7). This means that we must be very careful to make definite predictions. But the p_T cutoff method seems to be a good alternative to the Monte Carlo simulation and Fig. 7 may be compared with experiments.

Note that the characteristic features in the x_H dependence and the relative importance between the QCD and direct-photon contributions are not changed very much by the cutoff effect. Where x_H is large the direct-photon contribution is dominant, whereas at smaller x_H it tends to be suppressed and we can clearly see the enhanced

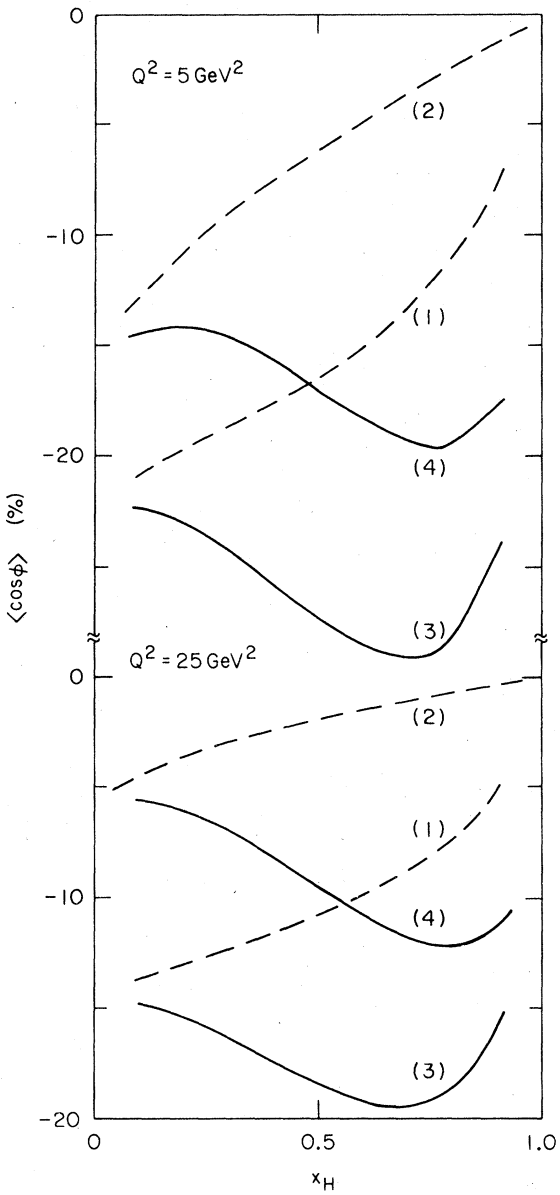

FIG. 6. The x_H dependence of $\langle\cos\phi\rangle$ without p_T cutoff. (1) QCD. (2) NPM with $\langle k_T^2\rangle = (400\ \text{MeV})^2$. (3) QCD + "direct photon". (4) NPM [as in (2)] + direct photon.

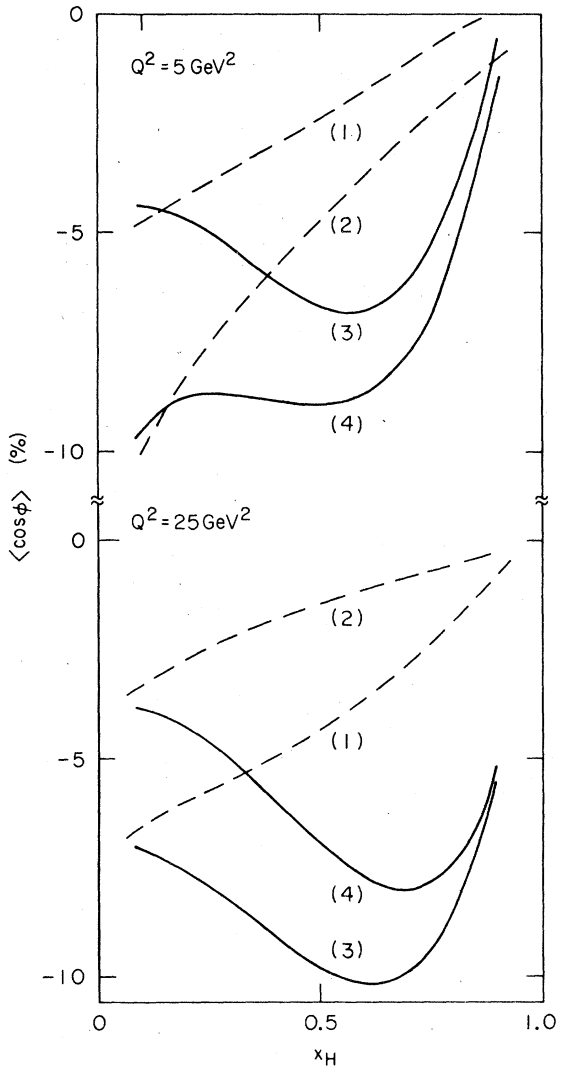

FIG. 7. The x_H dependence of $\langle \cos\phi \rangle$ with the condition $p_T \geq 300$ MeV. (1) QCD. (2) NPM with $\langle k_T^2 \rangle = (400\ \text{MeV})^2$. (3) QCD + direct photon. (4) NPM [as in (2)] + direct photon.

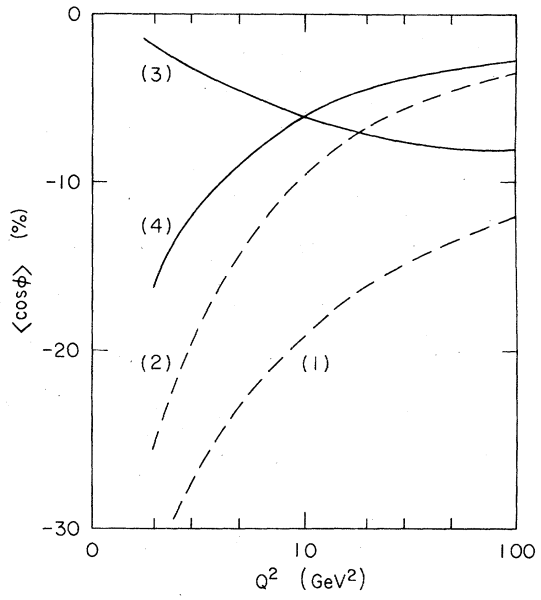

FIG. 8. The Q^2 dependence of $\langle \cos\phi \rangle$ at $x_H = 0.2$. (1) QCD + direct photon without p_T cutoff. (2) NPM + direct photon without p_T cutoff. (3) QCD + direct photon with $p_T \geq 300$ MeV. (4) NPM + direct photon with $p_T \geq 300$ MeV.

QCD effects. In particular, around $x_H \simeq 0.2$, $\langle \cos\phi \rangle$ is overwhelmingly dominated by the QCD contribution.

To discriminate the QCD effect from the k_T effect of NPM, the Q^2 dependence is helpful (see Fig. 8). QCD with p_T cutoff predicts gradually increasing $|\langle \cos\phi \rangle|$ with Q^2 (though it is mainly due to the p_T cutoff), whereas NPM with VMD predicts $|\langle \cos\phi \rangle|$ to decrease rapidly with increasing Q^2.

The asymmetry $\langle \cos 2\phi \rangle$ arises predominantly from the direct-photon contribution and is insensitive to p_T cutoff (compare Figs. 9 and 10). Thus its absolute value is a reliable prediction. For the reasons stated before, the values with p_T cutoff (i.e., Fig. 10) are to be more realistic. $\langle \cos 2\phi \rangle$ has little to do with the QCD test, but it is certainly worthwhile comparing experimental results with our calculations since it will verify the direct-photon coupling very clearly. Its Q^2 dependence with a fixed $x_H = 0.2$ is shown in Fig. 11.

The cross sections are shown in Figs. 12 and 13.

There might be disturbances to azimuthal asymmetries due to fluctuation of parton k_T as in Drell-Yan processes[24] which appears to be caused by soft-gluon bremsstrahlung. If there should be these disturbances, our result for $\langle \cos\phi \rangle$ would be changed. ($\langle \cos 2\phi \rangle$ would not change because it came mainly from the direct-photon contribution.) But even if these effects were contributing, we could get rid of them by changing the experimental determination of ϕ. We suggest disregarding the momentum axis of the virtual photon and the target electron (or positron) in determining the hadron plane. A possible choice of ϕ is the following:

(1) In the frame where $q^0 = 0$ and $\vec{q} \parallel \vec{P}$ (= momentum of the target electron or positron), select those hadrons of momentum p which satisfies the condition $\vec{p} \cdot \vec{q} > 0$ (which means "not emitted in the forward hemisphere of the target").

(2) Define $P_{\text{sum}} \equiv \sum_i p^{(i)}$, where the summation is over all hadrons selected in (1).

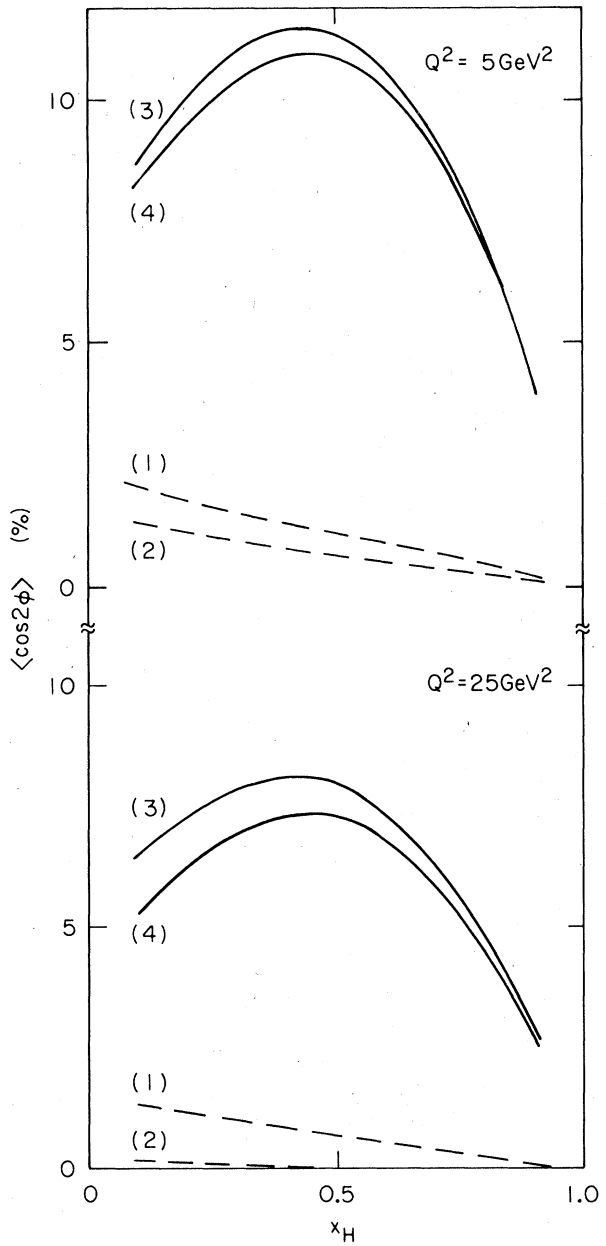

FIG. 9. The x_H dependence of $\langle \cos 2\phi \rangle$ without p_T cut-off. (1) QCD. (2) NPM with $\langle k_T^2 \rangle = (400\ \mathrm{MeV})^2$. (3) QCD + direct photon. (4) NPM [as in (2)] + direct photon.

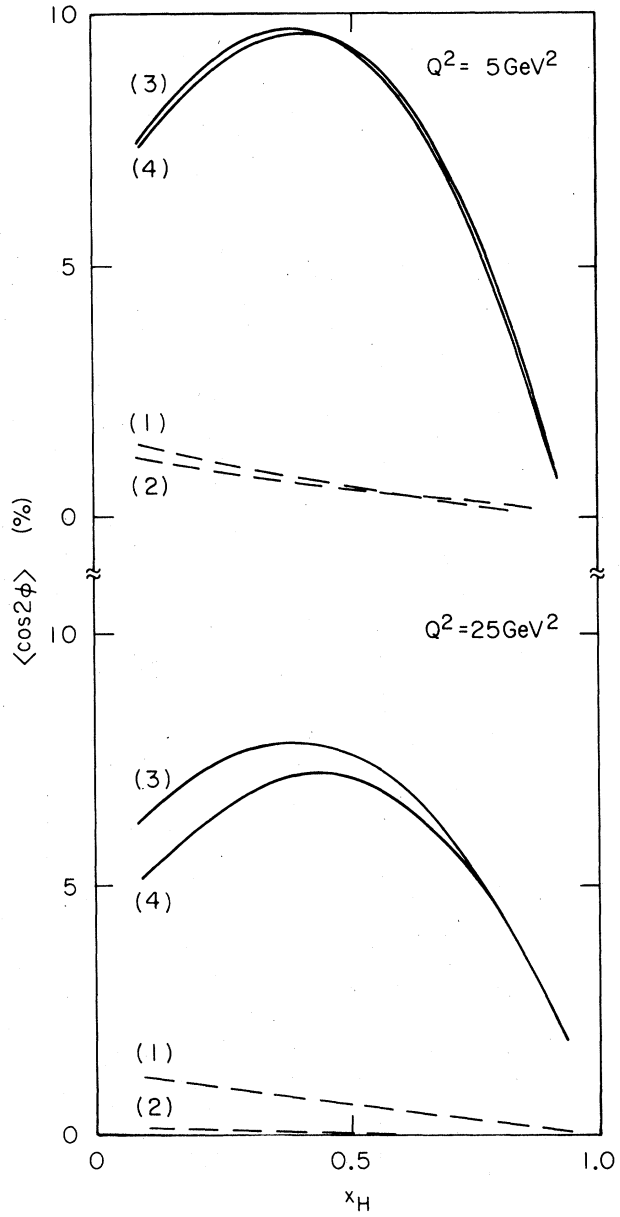

FIG. 10. The x_H dependence of $\langle \cos 2\phi \rangle$ with the condition $p_T \geq 300$ MeV. (1) QCD. (2) NPM with $\langle k_T^2 \rangle = (400\ \mathrm{MeV})^2$. (3) QCD + direct photon. (4) NPM [as in (2)] direct photon.

(3) In the frame with $q^0 = 0$ and $\vec{q} \| \vec{P}_{sum}$ (not $\vec{P}$), determine ϕ following the same procedure as that suggested previously, but replacing P by $P' = (|\vec{P}_{sum}|, -\vec{P}_{sum})$ in (4.1).

This method is related to the following calculational constraints of $x_p > \frac{1}{2}$ and $z_p' < x_p$ in the previous calculations. That is, only those events satisfying these constraints contribute to the azimuthal asymmetries of the new ϕ.

Another merit of the above definition of ϕ is that we can single out as the pure direct-photon events satisfying the conditions $x_p > \frac{1}{2}$ and $z_p' < x_p$ those events without any jets in the forward hemisphere of the target electron (or positron). We call those events accompanying a forward jet "the QCD events". (Actually this class of events contains some direct-photon events which are not counted

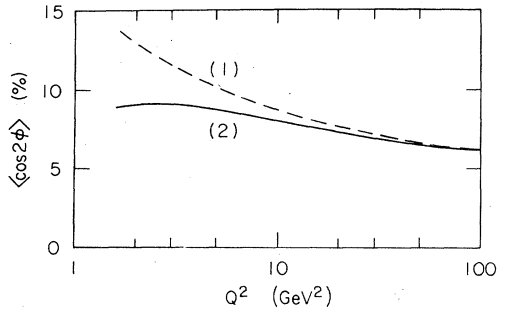

FIG. 11. The Q^2 dependence of $\langle \cos 2\phi \rangle$ at $x_H = 0.2$. (1) QCD + direct photon without p_T cutoff. (2) QCD + direct photon with $p_T \geq 300$ MeV.

in the above selection.) We could measure the angular asymmetries of each category of events independently. In the direct-photon events P' will be parallel to P in almost all events because the characteristic value of k_T of the target virtual photon is of the order of electron mass. So we can safely use P instead of the elaborately defined P'.

In the following we present our results for the

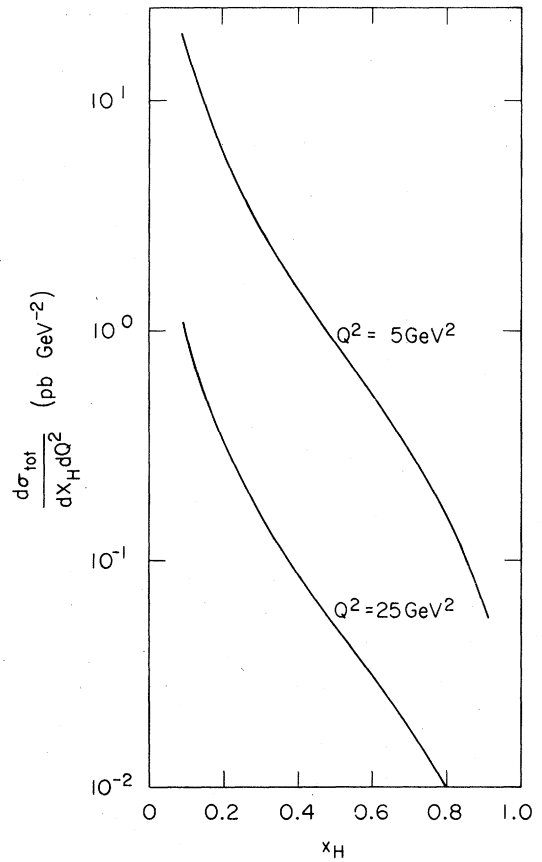

FIG. 12. The x_H dependence of the total cross section for electron deep-inelastic scattering ($\sqrt{s} = 100$ GeV).

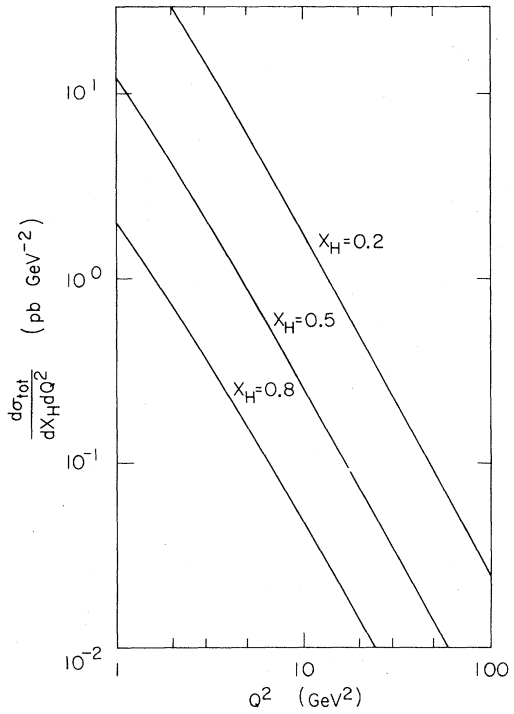

FIG. 13. The Q^2 dependence of the total cross section for electron deep-inelastic scattering ($\sqrt{s} = 100$ GeV).

azimuthal asymmetries with respect to the newly defined ϕ. We show the results without p_T cutoff in Fig. 14 and those with p_T cutoff requiring $p_T \geq 300$ MeV in Fig. 15. $\langle \cos 2\phi \rangle$ of the QCD events may be too small to be detected. $\langle \cos\phi \rangle$ is again sensitive to p_T cutoff and that of the QCD events after the cutoff is small as shown in Fig. 15. (If the effective p_T cutoff due to the hadronization is to be smaller, it will of course be more enhanced.) For the direct-photon events both $\langle \cos\phi \rangle$ and $\langle \cos 2\phi \rangle$ seem to be large enough for their detection. (The increase of $\langle \cos 2\phi \rangle$ after the p_T cutoff is due to the drop of the direct-photon cross section with p_T cutoff and is somewhat artificial.)

The Q^2 dependence of the azimuthal asymmetries is shown in Figs. 16 and 17 for various cases.

The cross sections for the direct-photon events are shown in Fig. 18.

V. CONCLUSIONS AND REMARKS

The photon structure functions are studied in the framework of Curci, Furmanski, and Petronzio. A focus is given on the renormalization mechanism of the collinear mass singularities in the case of the target photon. The electron structure functions can be studied on equal footing due to the equivalent-photon approximation.

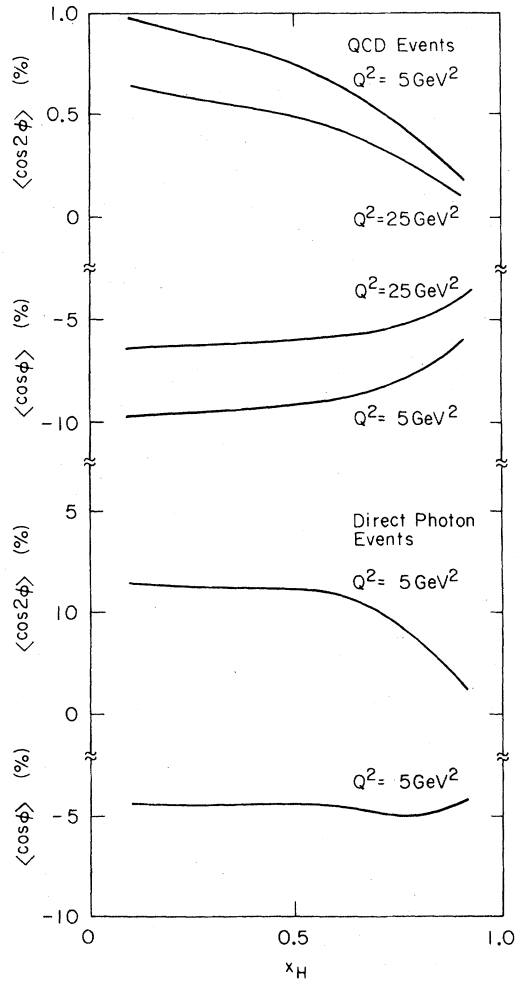

FIG. 14. The x_H dependence of the azimuthal asymmetries with the improved definition of ϕ (without p_T cutoff). As to the direct-photon events, the result is almost Q^2 independent.

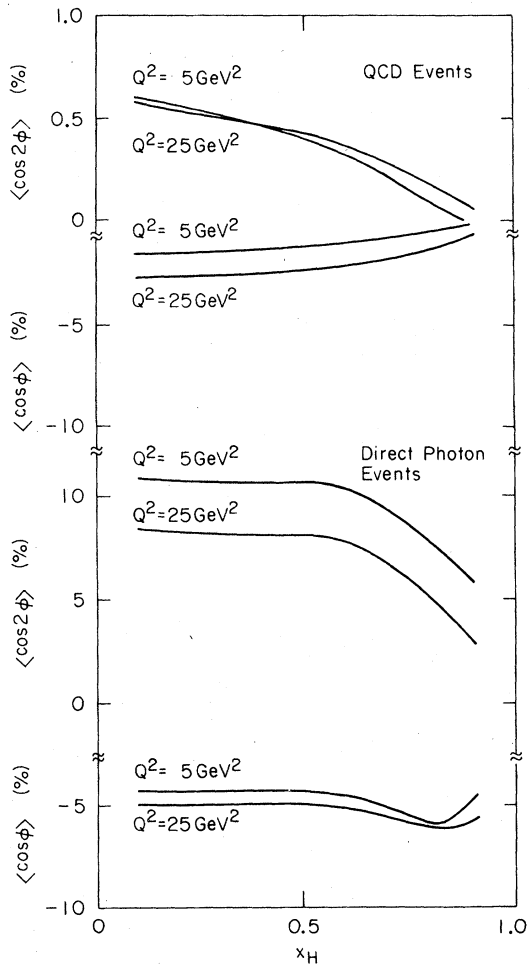

FIG. 15. The x_H dependence of the azimuthal asymmetries with the improved definition of ϕ (with the condition $p_T \geq 300$ MeV).

Then the azimuthal asymmetries in the deep-inelastic e^+e^- scattering are investigated. The detailed results are shown in Figs. 6–11. $\langle\cos\phi\rangle$ is large but expected to be diminished considerably in hadronization processes. We take this effect into account phenomenologically by requiring the p_T cutoff of $p_T \geq 300$ MeV. The signals and characteristics of $\langle\cos\phi\rangle$ seems to be enough to be detected. Its Q^2 dependence will be helpful to distinguish QCD from NPM. $\langle\cos 2\phi\rangle$ is large and not expected to be diminished much in hadronization processes. It serves as a very good test for the direct-photon contributions in the photon deep-inelastic scattering.

The method is suggested to get rid of possible backgrounds due to parton k_T from soft-gluon emission or from any other mechanism. In this method $\langle\cos\phi\rangle$ of the QCD events is diminished and seems difficult to detect. Their $\langle\cos 2\phi\rangle$ detection is likely to be harder. On the other hand, $\langle\cos\phi\rangle$ and $\langle\cos 2\phi\rangle$ of the direct-photon events (i.e., events with no forward jet of the target electron or positron) turn out to be large and we conclude that they can provide clean signals for the direct-photon process.

Finally, we remark that the higher-order corrections and the inclusion of charm quark effects are left as future problems.

ACKNOWLEDGMENTS

One of the authors (A. H.) wishes to thank K. I. Aoki for discussions and comments. Another author (J. K.) is grateful to the Theory Group at SLAC for their kind hospitality. This work was supported in part by the Department of Energy

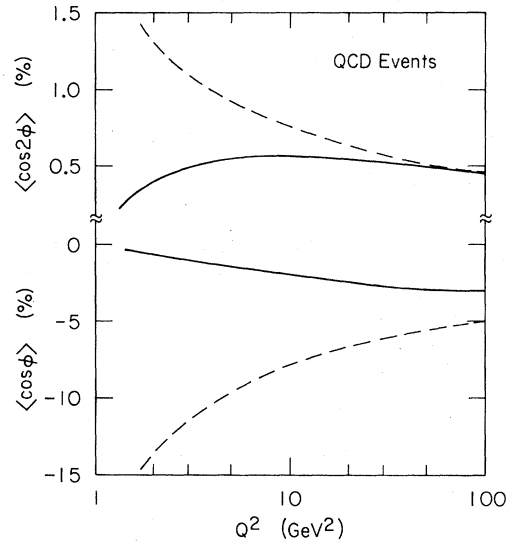

FIG. 16. The Q^2 dependence of the azimuthal asymmetries for the QCD events ($x_H = 0.2$). Dashed line: without p_T cutoff. Solid line: with $p_T \geq 300$ MeV.

under Contract No. DE-AC03-76SF00515 and by the Japan Society for the Promotion of Science through the Joint Japan-U. S. Collaboration in High Energy Physics.

APPENDIX A: ANOMALOUS DIMENSIONS

We list the expressions for the anomalous dimensions which appeared in the text:

$$d_N^{\mathrm{NS}} = \frac{C_2(R)}{\beta_0}\left[1 - \frac{2}{N(N+1)} + 4\sum_{l=2}^{\infty}\left(\frac{1}{l} - \frac{1}{l+N-1}\right)\right]$$

(NS indicates nonsinglet),

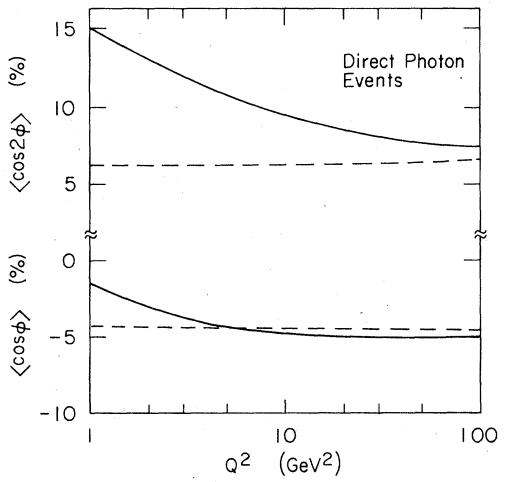

FIG. 17. The Q^2 dependence of the azimuthal asymmetries for the direct-photon events ($x_H = 0.2$). Dashed line: without p_T cutoff. Solid line: with $p_T \geq 300$ MeV.

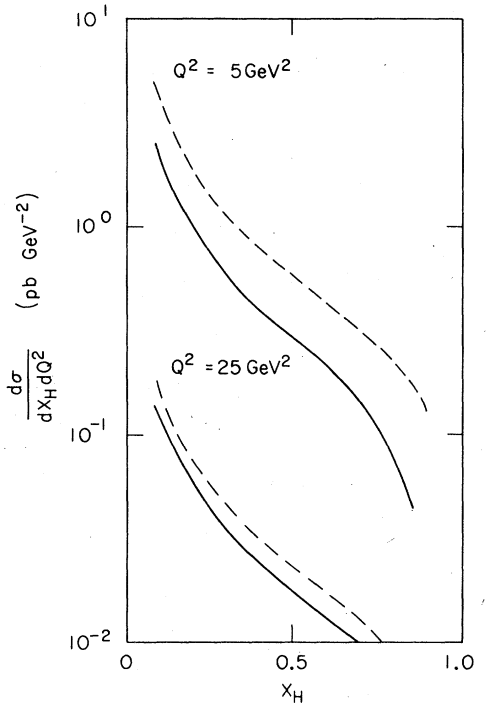

FIG. 18. The x_H dependence of the cross section for the direct-photon events. Dashed line: without p_T cutoff. Solid line: with $p_T \geq 300$ MeV.

$$d_N^{qG} = \frac{4T(R)}{\beta_0}\frac{2+N+N^2}{N(N+1)(N+2)},$$

$$d_N^{Gq} = \frac{2C_2(R)}{\beta_0}\frac{2+N+N^2}{N(N^2-1)},$$

$$d_N^{GG} = \frac{C_2(G)}{\beta_0}\left[\frac{1}{3} - \frac{4}{N(N-1)} - \frac{4}{(N+1)(N+2)} + 4\sum_{l=2}^{\infty}\left(\frac{1}{l} - \frac{1}{l+N-1}\right) + \frac{4T(R)}{3C_2(R)}\right],$$

$$d_N^{q\gamma} = \frac{2+N+N^2}{N(N+1)(N+2)},$$

$$d_N^{\pm} = \frac{1}{2}\left\{(d_N^{\mathrm{NS}} + d_N^{GG}) \pm \left[(d_N^{\mathrm{NS}} - d_N^{GG})^2 + d_N^{qG}\, d_N^{Gq}\right]^{1/2}\right\},$$

where

$$\beta_0 = \tfrac{11}{3}C_2(G) - \tfrac{4}{3}T(R)$$

and

$$C_2(R) = \frac{N^2-1}{2N}, \quad T(R) = \frac{f}{2}, \quad C_2(G) = N$$

for SU(N) color gauge group with f flavors.

APPENDIX B: CALCULATION OF PARTON CROSS SECTIONS

The calculation is most easily done in the frame where $q^0 = 0$ and $\vec{q} \parallel \vec{p}_1$. We define the unit vectors

in this frame as follows:

$$\epsilon_L^\mu = \frac{\bar{q}^\mu}{|\vec{\bar{q}}|}, \quad \epsilon_0^\mu = (1,0,0,0), \quad \epsilon_T^\mu = \frac{\bar{k}_1^\mu + \bar{k}_2^\mu}{|\vec{k}_1 + \vec{k}_2|}$$

and

$$\epsilon_s \cdot \epsilon_i = 0, \quad \epsilon_s^2 = -1 \quad (i = 0, T, L) \tag{B1}$$

with

$$\bar{q}^\mu = (0, \vec{q}), \quad \bar{k}_1^\mu + \bar{k}_2^\mu = (0, \vec{k}_1 + \vec{k}_2). \tag{B2}$$

Defining the leptonic tensor

$$\langle L^{\mu\nu} \rangle_{\text{spin}} = \tfrac{1}{2} \text{Tr}(\not{k}_1 \gamma^\mu \not{k}_2 \gamma^\nu), \tag{B3}$$

we find

$$\frac{\langle L^{\mu\nu} \rangle_{\text{spin}}}{Q^2} = \frac{4(1-y)}{y^2} \epsilon_0^\mu \epsilon_0^\nu + \frac{1+(1-y)^2}{y^2} (\epsilon_T^\mu \epsilon_T^\nu + \epsilon_s^\mu \epsilon_s^\nu) + \frac{2(2-y)(1-y)^{1/2}}{y^2} (\epsilon_0^\mu \epsilon_T^\nu + \epsilon_T^\mu \epsilon_0^\nu) + \frac{2(1-y)}{y^2} (\epsilon_T^\mu \epsilon_T^\nu - \epsilon_s^\mu \epsilon_s^\nu). \tag{B4}$$

We define the hadronic tensor

$$\langle W_{\mu\nu} \rangle_{\text{spin}} = \langle p_1 | J_\mu(0) | p_2, p_3 \rangle \langle p_2, p_3 | J_\nu(0) | p_1 \rangle \tag{B5}$$

with the normalization

$$\langle p | p' \rangle = (2\pi)^3 2p^0 \delta^3(\vec{p} - \vec{p}'). \tag{B6}$$

The cross section is then given by

$$d\sigma = \frac{1}{4 p_1 \cdot k_1} \frac{d^3k_2}{(2\pi)^3 2k_2^0} \frac{d^3p_2}{(2\pi)^3 2p_2^0} \frac{d^3p_3}{(2\pi)^3 2p_3^0} \frac{(4\pi\alpha_{\text{em}})^2 e_q^2}{Q^4} \times \langle L^{\mu\nu} \rangle_{\text{spin}} \langle W_{\mu\nu} \rangle_{\text{spin}} (2\pi)^4 \delta^4(k_1 + p_1 - k_2 - p_2 - p_3)$$

$$= \frac{1}{4 p_1 \cdot k_1} \frac{d^3k_2}{(2\pi)^3 2k_2^0} \frac{d^3p_2}{(2\pi)^3 2p_2^0} \frac{(4\pi\alpha_{\text{em}})^2 e_q^2}{Q^2} \frac{\langle L^{\mu\nu} \rangle_{\text{spin}}}{Q^2} \times \langle W_{\mu\nu} \rangle_{\text{spin}} (2\pi) \delta^+((p_1 + q - p_2)^2) \Big|_{q = k_1 - k_2}. \tag{B7}$$

Since we have

$$\delta^+((p_1 + q - p_2)^2) = z_p \delta\left(p_T^2 - \frac{z_p}{x_p} (1 - x_p)(1 - z_p) Q^2 \right), \tag{B8}$$

$$\frac{d^3p_2}{(2\pi)^3 2p_2^0} = \frac{dp_T^2 dz_p d\phi}{(2\pi)^3 4 z_p}, \tag{B9}$$

$$\frac{d^3k_2}{(2\pi)^3 2k_2^0} = \pi p_1 \cdot k_1 \frac{y\, dy\, dx_p}{(2\pi)^3}, \tag{B10}$$

we finally obtain

$$\frac{d\sigma}{dx_p dy dz_p dp_T^2 d\phi} = \frac{\alpha_{\text{em}}^2 e_q^2}{32\pi^2} \frac{y}{Q^2} \frac{\langle L^{\mu\nu} \rangle_{\text{spin}}}{Q^2} \langle W_{\mu\nu} \rangle_{\text{spin}} \times \delta\left(p_T^2 - \frac{z_p}{x_p} (1 - x_p)(1 - z_p) Q^2 \right). \tag{B11}$$

When the initial parton is a quark, we find

$$\langle W^{\mu\nu} \rangle_{\text{spin}}^q = g_s^2(Q^2) C_2(R) \frac{-2q^2}{(p_1 \cdot p_3)(p_2 \cdot p_3)} \left[\left(p_1^\mu - \frac{p_1 \cdot q}{q^2} q^\mu \right) \left(p_1^\nu - \frac{p_1 \cdot q}{q^2} q^\nu \right) + (p_1 \leftrightarrow p_2) + \frac{(p_1 \cdot q)^2 + (p_2 \cdot q)^2}{q^2} \left(g^{\mu\nu} - \frac{q^\mu q^\nu}{q^2} \right) \right]$$

$$= 4\pi\alpha_s(Q^2) C_2(R) \frac{4x_p}{(1 - x_p)(1 - z_p)} \left[2x_p \frac{p_1^\mu p_1^\nu + p_2^\mu p_2^\nu}{Q^2} - \frac{2x_p z_p + (1 - z_p)^2 + (1 - x_p)^2}{2x_p} g^{\mu\nu} + (\text{terms proportional to } q^\mu, q^\nu) \right]. \tag{B12}$$

For a gluon as the initial parton, we have

$$\langle W^{\mu\nu} \rangle_{\text{spin}}^G = g_s^2(Q^2) T(R) \frac{-2q^2}{(p_1 \cdot p_2)(p_1 \cdot p_3)} \left[\left(p_2^\mu - \frac{p_2 \cdot q}{q^2} q^\mu \right) \left(p_2^\nu - \frac{p_2 \cdot q}{q^2} q^\nu \right) + (p_2 \leftrightarrow p_3) + \frac{(p_2 \cdot q)^2 + (p_3 \cdot q)^2}{Q^2} \left(g^{\mu\nu} - \frac{q^\mu q^\nu}{q^2} \right) \right]$$

$$= 4\pi\alpha_s(Q^2) T(R) \frac{4x_p}{z_p(1 - z_p)} \left[2x_p \frac{p_2^\mu p_2^\nu + p_3^\mu p_3^\nu}{C^2} - \frac{1 - 2(z_p(1 - z_p) + x_p(1 - x_p))}{2x_p} g^{\mu\nu} + (\text{terms proportional to } q^\mu, q^\nu) \right].$$

Using the relations

$$p_2^\mu = \frac{Q}{2x_p}[(1-x_p)(1-z_p)+x_p z_p]\epsilon_0^\mu + \frac{Q}{2}\left(1-\frac{1-z_p}{x_p}\right)\epsilon_L^\mu + Q\left[\frac{z_p}{x_p}(1-z_p)(1-x_p)\right]^{1/2}\cos\phi\,\epsilon_T^\mu$$
$$+Q\left[\frac{z_p}{x_p}(1-z_p)(1-x_p)\right]^{1/2}\sin\phi\,\epsilon_s^\mu , \tag{B14}$$

$$p_3^\mu = \frac{Q}{2x_p}[x_p(1-z_p)+z_p(1-x_p)]\epsilon_0^\mu + \frac{Q}{2}\left(1-\frac{z_p}{x_p}\right)\epsilon_L^\mu - Q\left[\frac{z_p}{x_p}(1-z_p)(1-x_p)\right]^{1/2}\cos\phi\,\epsilon_T^\mu$$
$$-Q\left[\frac{z_p}{x_p}(1-z_p)(1-x_p)\right]^{1/2}\sin\phi\,\epsilon_s^\mu , \tag{B15}$$

we obtain the formulas in Sec. III.

If we calculate with scalar gluons, (B12) becomes

$$\langle W^{\mu\nu}\rangle_{\text{spin}}^{\text{scalar}} \propto g^2\,\frac{-q^2}{(p_1\cdot p_3)(p_2\cdot p_3)}\left[\left(p_3^\mu - \frac{p_3\cdot q}{q^2}q^\mu\right)\left(p_3^\nu - \frac{p_3\cdot q}{q^2}q^\nu\right) + \frac{(p_3\cdot q)^2}{q^2}\left(g^{\mu\nu}-\frac{q^\mu q^\nu}{q^2}\right)\right]$$

$$\propto g^2\frac{2x_p}{(1-x_p)(1-z_p)}\left[2x_p\frac{p_3^\mu p_3^\nu}{Q^2} - \frac{(z_p-x_p)^2}{2x_p}g^{\mu\nu} + (\text{terms proportional to } q^\mu, q^\nu)\right] . \tag{B16}$$

[1] R. K. Ellis, H. Georgi, M. Machacek, H. D. Politzer, and G. G. Ross, Phys. Lett. 78B, 281 (1978); Nucl. Phys. B152, 285 (1979).

[2] S. J. Brodsky *et al.*, Phys. Rev. Lett. 27, 280 (1971); H. Terazawa, Rev. Mod. Phys. 45, 615 (1973); V. Budnev *et al.*, Phys. Rep. 15C, 181 (1975).

[3] T. F. Walsh and P. Zerwas, Phys. Lett. 44B, 195 (1973); R. L. Kingsley, Nucl. Phys. B60, 45 (1973); R. P. Worden, Phys. Lett. 51B, 57 (1974); 52B, 87 (1974); M. A. Ahmed and G. G. Ross, *ibid.* 59B, 369 (1975).

[4] E. Witten, Nucl. Phys. B120, 189 (1977).

[5] C. H. Llewellyn Smith, Phys. Lett. 79B, 83 (1978).

[6] S. J. Brodsky, T. DeGrand, J. Gunion, and J. Weis, Phys. Rev. Lett. 41, 672 (1978); Phys. Rev. D 19, 1418 (1979).

[7] R. J. DeWitt, L. M. Jones, J. D. Sullivan, D. E. Willen, and H. H. Wyld, Phys. Rev. D 19, 2046 (1979); 20, 1751 (E) (1979).

[8] W. R. Frazer and J. F. Gunion, Phys. Rev. D 19, 2447 (1979); D 20, 147 (1979).

[9] K. Kajantie, Acta Phys. Austriaca, Suppl. XXI, 663 (1979).

[10] W. A. Bardeen and A. J. Buras, Phys. Rev. D 20, 166 (1979); 21, 1041 (E) (1980); K. Sasaki, *ibid.* 22, 2143 (1980); M. Abud, R. Gatto, and C. A. Savoy, *ibid.* 20, 2224 (1979); R. N. Cahn and J. F. Gunion, *ibid.* 20, 2253 (1979); K. Kajantie and R. Raitio, Phys. Lett. 87B, 133 (1979); Nucl. Phys. B159, 528 (1979); M. Lehto, University of Helsinki Report No. HU-TFT-80-12 (unpublished); J. Field, E. Pietarinen, and K. Kajantie, Nucl. Phys. B171, 377 (1980); A. DeVote *et al.*, Phys. Lett. 90B, 436 (1980); F. A. Berends, Z. Kunszt, and R. Gastmans, *ibid.* 92B, 186 (1980); Nucl. Phys. B182, 397 (1981); M. K. Chase, Nucl. Phys. B167, 125 (1980); K. Köller, T. F. Walsh, and P. M. Zerwas, Z. Phys. C2, 197 (1979); C. Peterson, T. F. Walsh, and P. M. Zerwas, Nucl. Phys. B174, 424 (1980).

[11] G. Curci, W. Furmanski, and R. Petronzio, Nucl. Phys. B175, 27 (1980); W. Furmanski and R. Petronzio, Phys. Lett. 97B, 437 (1980).

[12] H. Georgi and H. Politzer, Phys. Rev. Lett. 40, 3 (1978).

[13] R. N. Cahn, Phys. Lett. 78B, 269 (1978).

[14] R. P. Feynman, *Photon-Hadron Interactions* (Benjamin, New York, 1972).

[15] P. Binétruy and G. Girardi, Nucl. Phys. B155, 169 (1979).

[16] E. C. G. Stueckelberg and A. Peterman, Helv. Phys. Acta 26, 499 (1953); M. Gell-Mann and F. Low, Phys. Rev. 95, 1300 (1954).

[17] T. Kinoshita, J. Math. Phys. 3, 650 (1962); T. D. Lee and M. Nauenberg, Phys. Rev. 133, 1549 (1964).

[18] H. Politzer, Nucl. Phys. B129, 301 (1977).

[19] G. Altarelli and G. Parisi, Nucl. Phys. B126, 298 (1977).

[20] A. Méndez, Nucl. Phys. B145, 199 (1978).

[21] A. De Rújula, J. Ellis, E. G. Floratos, and M. K. Gaillard, Nucl. Phys. B138, 387 (1978).

[22] C. T. Hill and G. G. Ross, Nucl. Phys. B148, 373 (1979).

[23] See also C. Tao *et al.*, Phys. Rev. Lett. 44, 1726 (1980).

[24] G. Parisi and R. Petronzio, Nucl. Phys. B154, 427 (1979).